pubs.acs.org/acschemicalbiology

Articles

Short FcRn-Binding Peptides Enable Salvage and Transcytosis of scFv Antibody Fragments

Vince W. Kelly and Shannon J. Sirk*

Cite This: *ACS Chem. Biol.* 2022, 17, 404–413

Read Online

ACCESS | Metrics & More | Article Recommendations | Supporting Information

ABSTRACT: Therapeutic antibodies have become one of the most widely used classes of biotherapeutics due to their unique antigen specificity and their ability to be engineered against diverse disease targets. There is significant interest in utilizing truncated antibody fragments as therapeutics, as their small size affords favorable properties such as increased tumor penetration as well as the ability to utilize lower-cost prokaryotic production methods. Their small size and simple architecture, however, also lead to rapid blood clearance, limiting the efficacy of these potentially powerful therapeutics. A common approach to circumvent these limitations is to enable engagement with the half-life extending neonatal Fc receptor (FcRn). This is usually achieved via fusion with a large Fc domain, which negates the benefits of the antibody fragment's small size. In this work, we show that modifying antibody fragments with short FcRn-binding peptide domains that mimic native IgG engagement with FcRn enables binding and FcRn-mediated recycling and transmembrane transcytosis in cell-based assays. Further, we show that rational, single amino acid mutations to the peptide sequence have a significant impact on the receptor-mediated function and investigate the underlying structural basis for this effect using computational modeling. Finally, we report the identification of a short peptide from human serum albumin that enables FcRn-mediated function when grafted onto a single-chain variable fragment (scFv) scaffold, establishing an approach for the rational selection of short-peptide domains from full-length proteins that could enable the transfer of non-native functions to small recombinant proteins without significantly impacting their size or structure.

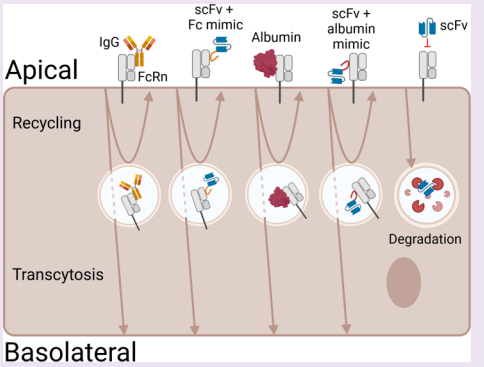

INTRODUCTION

Over the past several decades, antibody-based drugs have been developed to treat a number of diverse diseases. With an ever-expanding market and steady pace of product approvals,[1] the therapeutic and economic impact of this class of drugs continues to grow as researchers further engineer these complex biomolecules to improve performance and decrease cost. Many of these efforts have advanced to clinical use,[2−4] including the generation of antibody−drug conjugates to enhance potency,[5] the fusion of select antibody domains to improve the pharmacokinetics of active biologicals,[6] and the development of engineered antibody fragments for imaging[7] and therapy.[8,9] Due to their size, small antibody fragments, in particular, offer a number of advantages over larger, full-length antibodies, including improved tissue penetration and more efficient and cost-effective production in prokaryotic systems.[10,11]

Despite these advantages, the therapeutic development of small antibody fragments remains particularly challenging compared to that of full-length antibodies because, to reduce size, most fragments lack an Fc (crystallizable fragment) domain. In addition to mediating immune effector functions such as recruiting humoral and cellular responses,[12] the Fc domain is also responsible for extending the serum half-life of antibodies via engagement with the neonatal Fc receptor (FcRn), promoting recycling rather than degradation of these long-lived serum proteins (Figure 1A).[13,14] FcRn also binds albumin in a similar way (but at an orthogonal binding site) (Figure 1B). When IgG or albumin is taken up by polarized epithelial or endothelial cells, they are packaged into endosomes, which acidify as they traffic through the cell.[15] In this low-pH environment, histidines on albumin and the IgG Fc domain are protonated and binding to FcRn and its cognate light-chain β2 microglobulin (β2m) is enabled.[16] Association of β2m with FcRn is required for binding with IgG and albumin. These albumin− or IgG−FcRn−β2m complexes are then trafficked away from the lysosomal fate and are either recycled back to the membrane from which they entered or transcytosed to the opposite membrane, where they are released upon encountering the physiological pH of the extracellular environment. Small antibody fragments lacking an Fc domain are unable to engage FcRn and are thus rapidly

Received: October 31, 2021
Accepted: January 10, 2022
Published: January 20, 2022

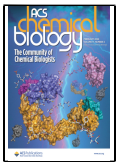

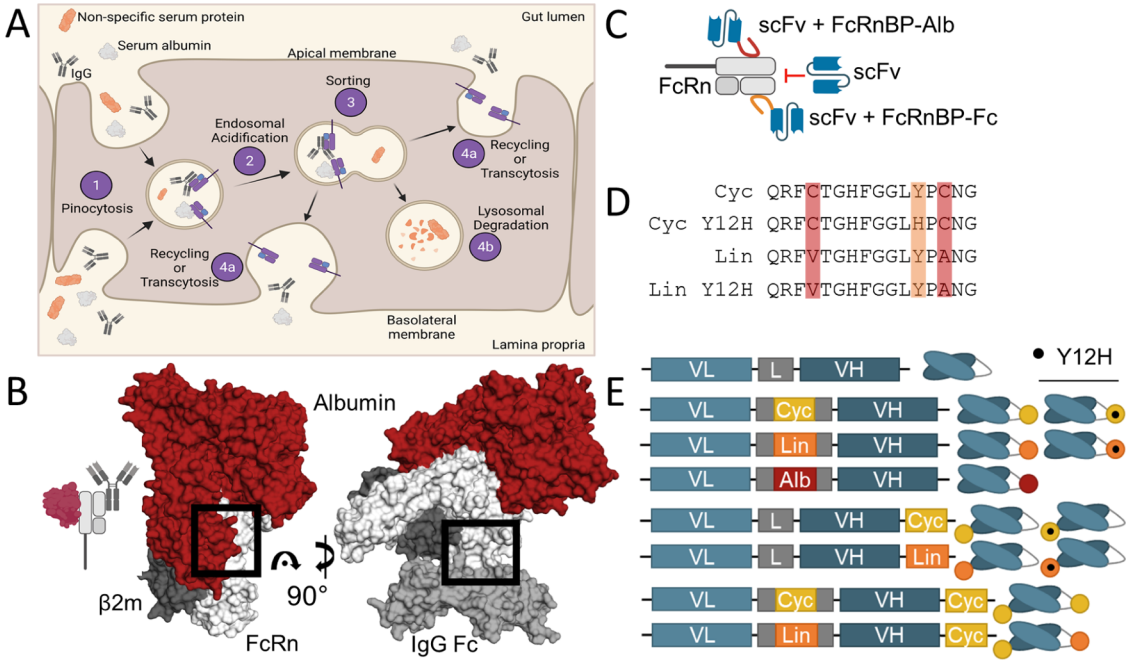

Figure 1. Neonatal Fc receptor engagement and scFv–peptide construction. (A) Schematic representation of FcRn-mediated transport: (1) proteins are taken up by pinocytosis at the apical or basolateral membrane and are packaged into endosomes; (2) endosomes acidify as they are trafficked through the cell, and the decrease in pH permits the binding of IgG and albumin to FcRn in the endosomal membrane; (3) endosomes are sorted toward or away from lysosomal fate; (4a) IgG and albumin bound to FcRn are either recycled to the membrane at which they were internalized or transcytosed to the opposite membrane; upon endosomal fusion with the cell membrane and exposure to the extracellular environment, increased pH causes protein release from FcRn; (4b) proteins not bound by FcRn are degraded in the lysosome. (B) Cartoon representation (left) and crystal structures (right) of human serum albumin (red) and IgG Fc (medium gray) in complex with FcRn (white) and β2m (dark gray). Black boxes denote binding interfaces. (C) Cartoon representation of the anticipated FcRn engagement. (D) Sequence alignment of FcRn-binding peptides mimicking the IgG–FcRn interaction. Cyclic mutations are highlighted in red, and Y12H mutation is highlighted in orange. (E) Schematic representation of all peptide-modified scFvs described in this study. VL, variable light domain; VH, variable heavy domain; L, linker [also shown as unlabeled gray boxes flanking linker peptides]; Cyc, cyclic peptide; Lin, linear peptide; and Alb, albumin peptide.

cleared from the circulation over several hours rather than persisting for several weeks as with full-length antibodies or native albumin.

In this work, we describe the development of antibody fragments engineered to engage FcRn via small peptide modifications that mimic the functionality of the FcRn-binding domains of IgG or albumin without dramatically increasing the size of the antibody fragment (Figure 1C). We show that short, 16 amino acid Fc- or albumin-mimetic peptides effectively enable FcRn binding and FcRn-mediated recycling and transport across polarized epithelial cell barriers when grafted onto a single-chain variable fragment (scFv) specific for human epidermal growth factor receptor 2 (HER2). HER2 is a highly studied target for therapeutic antibodies, thus providing a robust and well-characterized platform for the development of our approach. Together, our results reveal that the engineering and application of minimal peptides designed to mimic key physiological interactions is a promising approach for the functionalization of small antibody fragments, providing a means to cost-effectively increase the therapeutic efficacy and utility of this class of drug.

RESULTS AND DISCUSSION

Modification of Trastuzumab scFv with FcRn-Targeting Peptides. We selected trastuzumab[17] to establish our approach because it is exceptionally well characterized, providing a robust standard for evaluating our antibody fragments. We generated trastuzumab scFvs in the V_L–V_H orientation with a standard $(Gly_4Ser)_3$ linker. Previous studies using small peptides to enable the transepithelial transcytosis of larger proteins identified a series of 16 amino acid peptides that bind FcRn in a pH-dependent fashion.[18,19] These peptides have a mostly conserved consensus sequence, with two important variations: (1) replacement of Val4 and Ala14 with cysteines adds a disulfide bond and promotes a cyclic (Cyc) rather than linear (Lin) peptide conformation and (2) replacement of Tyr12 in the parental peptide with a His residue (Y12H) enhances pH-dependent binding to FcRn (Figure 1D). We constructed HER2-targeting scFv variants modified with each of these four peptide architectures (Cyc, CycY12H, Lin, LinY12H) in each of three orientations: as C-terminal extensions, as part of the linker connecting the V_H and V_L domains, or as both (Figure 1E), resulting in a collection of 12 modified variants. We were only able to generate four double-peptide variants (V_L-Cyc-V_H-Cyc, V_L-Lin-V_H-Cyc, V_L-CycY12H-V_H-Lin, and V_L-Lin-V_H-CycY12H) due to challenges with gene amplification of constructs containing duplicate copies of nearly identical peptides.

Building on the prior evidence that small peptide domains mimicking IgG Fc can enable FcRn-mediated interaction with fused proteins,[19] we sought to expand this approach by generating an alternative FcRn-binding peptide with orthogonal binding site specificity. Human serum albumin is known to interact extensively with FcRn, which promotes extended serum half-life,[20] and recent evidence has revealed that albumin is also robustly transported across polarized epithelia

https://doi.org/10.1021/acschembio.1c00862
ACS Chem. Biol. 2022, 17, 404–413

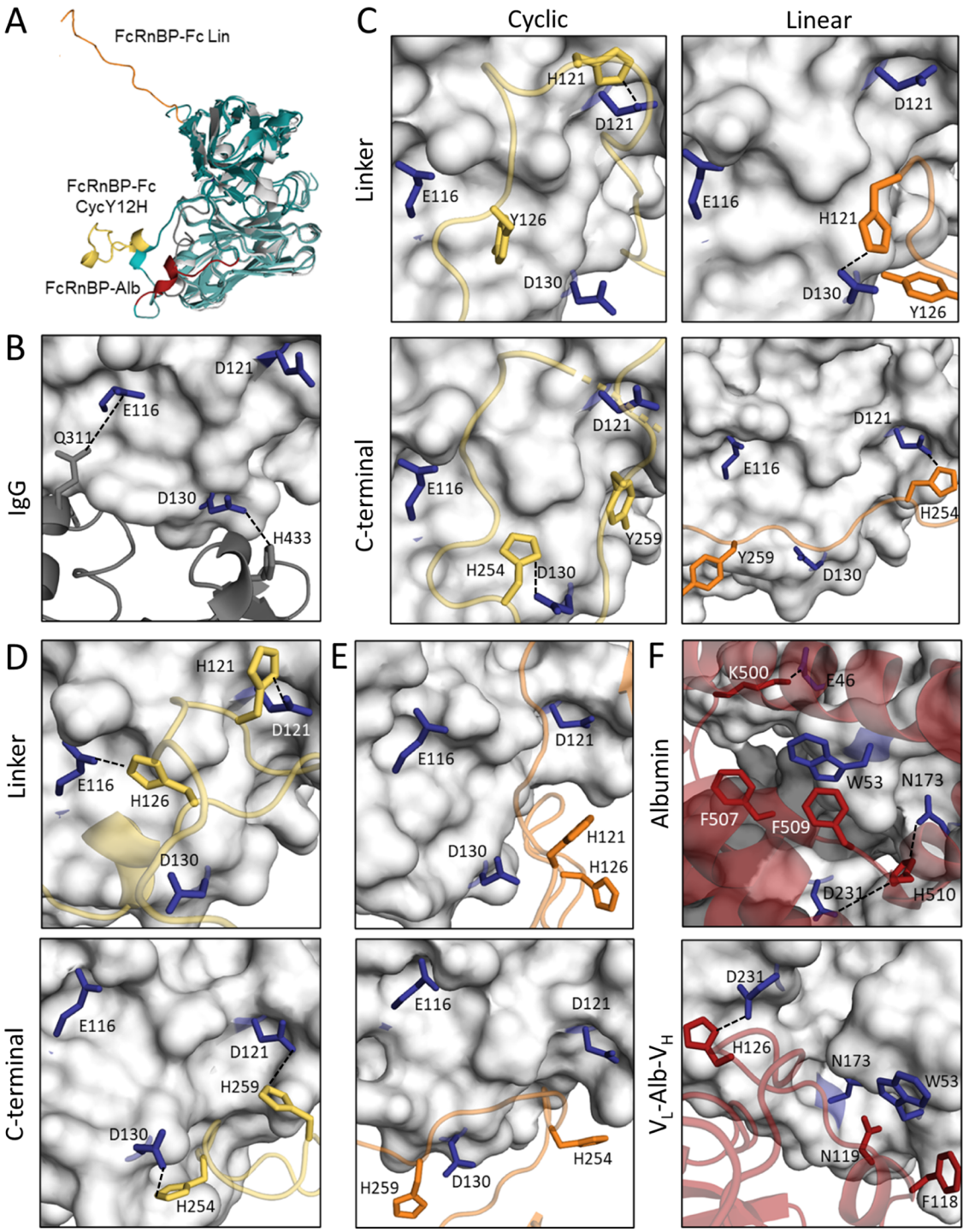

Figure 2. Computational modeling of the modified scFv structure and FcRn binding. (A) Crystal structure of an unmodified trastuzumab scFv (silver, PDB ID 6J71) overlayed with the modified trastuzumab scFvs. VL, cyan; VH, dark cyan; cyclic FcRnBP−Fc (linker, Y12H variant), gold; linear FcRnBP−Fc (C-terminal), orange; and FcRnBP−Alb (linker), red. (B) Crystal structure of the native IgG Fc−FcRn-binding interface. (C) Docking models of Cyc and Lin FcRnBP−Fc-modified scFvs with the FcRn/β2m complex. (D, E) Docking models of the FcRn/β2m complex with scFvs modified with (D) CycY12H FcRnBP−Fc and (E) LinY12H FcRnBP−Fc. (F) Docking models of human albumin (top) and an scFv modified with FcRnBP−Alb (bottom) with the FcRn/β2m complex. FcRn, white (key residues highlighted in blue); IgG, dark gray; Cyc FcRnBP−Fc, gold; Lin FcRnBP−Fc, orange; and albumin and albumin peptide, red.

by FcRn.[21] Further, albumin binds at a distinct site on FcRn and does not compete with IgG for binding (Figure 1B). We therefore selected albumin as a target protein for generating novel FcRn-binding peptide fusions. We examined the human albumin crystal structure (PDB 4N0U)[22] and identified a 14-amino acid stretch at the albumin−FcRn-binding interface (Tyr497−His510) with several similarities to the previously described FcRn-binding peptides, including a core hydrophobic residue (Phe509, 13, and 8 in albumin, albumin peptide, and Fc-mimic peptide, respectively) and a histidine in close proximity to acidic residues on FcRn. We grafted this peptide (FcRnBP−Alb) into the linker of our trastuzumab-

https://doi.org/10.1021/acschembio.1c00862
ACS Chem. Biol. 2022, 17, 404−413

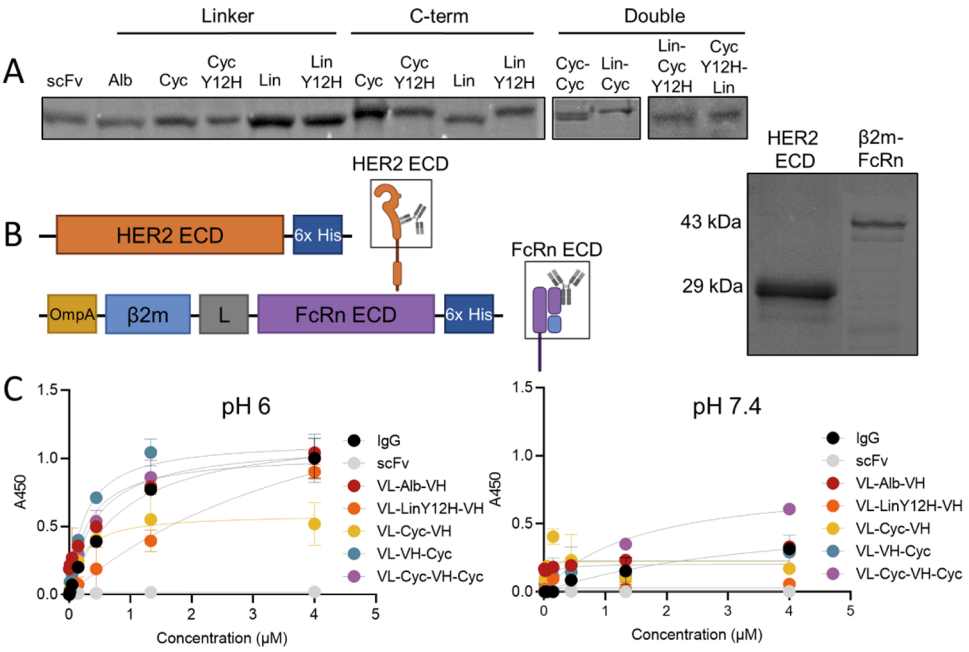

Figure 3. Recombinant protein expression and characterization. (A) SDS-PAGE of unmodified and peptide-modified scFvs used in this study; "scFv" indicates parental, unmodified trastuzumab scFv. (B) Schematic representation of the HER2 and FcRn–β2m fusion constructs used to produce the purified recombinant receptor extracellular domains (ECDs) and SDS-PAGE of purified ECDs. (C) Representative ELISA data from 5 of the 12 peptide-modified scFvs used in this study showing FcRn binding at pH 6 and 7.4, with unmodified scFv and full-length IgG controls. Assays were performed in triplicate. Error bars represent 1 standard deviation.

derived scFv, flanked by single-repeat Gly_4Ser spacers (Figure 1E).

Computational Modeling of scFv–Peptide Variant Structure and Binding to FcRn. To explore the impact of the peptide modifications on the structure of the scFvs, we used the Robetta webserver to generate predicted three-dimensional structures of scFv variants and then compared them to the unmodified trastuzumab scFv (PDB 6J71).[23] The results reveal minimal differences between the unmodified and modified structures, suggesting that the peptides do not impact the folding or overall structure of the scFvs (Figure 2A). We next used the model predictions with the lowest angstrom error estimate to perform molecular docking simulations with FcRn in its native heterodimeric conformation with β2m using the HADDOCK2.2 webserver[24] and compared the resulting models to the native Fc–FcRn complex (Figure 2B). Docked models revealed several key interactions between the canonical FcRn–Fc interface and FcRnBP–Fc variants. Most notably, histidine residues in both the intralinker (His121) and C-terminal (His254) Cyc and Lin FcRnBP–Fc make close contacts with FcRn residues Glu116 and Asp121, as well as Asp130, which is also involved in the interaction with full-length IgG[25] (Figure 2B,C). Furthermore, in docked models of variants with C-terminal or intralinker peptides containing both the cyclizing cysteine mutations (peptide positions V4C/A14C) and the acidifying Y12H mutation (His126 [linker] or 259 [C-term]), both of the peptide histidines (His121 and 126 [linker] or His254 and 259 [C-term]) form close contacts with acidic FcRn residues, as expected (Figure 2D). Conversely, models of linear FcRnBP–Fc reveal that the Y12H mutation leads to a kinked peptide conformation, increasing the distance between His121 or 254 and acidic FcRn residues Glu116, Asp121, and Asp130 and decreasing the predicted binding strength (Figure 2E). Docking simulations of FcRn with an FcRnBP–Alb-modified scFv also revealed key similarities with the native human albumin–FcRn interaction, including a close contact between Asp231 on FcRn with His510 on albumin that is mimicked by His126 on the FcRnBP–Alb-modified scFv and a hydrophobic interaction between FcRn Trp53 and Phe507 and 509 on albumin, which is mimicked by Phe118 on the FcRnBP–Alb-modified scFv (Figure 2F).

Protein Expression, Purification, and Characterization. We expressed all scFv variants into the periplasm of *E. coli* to facilitate proper folding and formation of internal disulfide bonds.[26] Protein yields for unmodified scFv and all FcRnBP-modified variants were ~3 to 5 mg/L of *E. coli* culture, suggesting that the peptide modifications do not negatively impact scFv folding or stability. SDS-PAGE analysis revealed expected shifts in molecular weight for all peptide-modified variants compared to those of the unmodified scFv (Figure 3A). We next assessed the ability of all scFv variants to bind their target antigen, HER2, by ELISA using a truncated HER2 extracellular domain[27] expressed and purified from *E. coli* (Figure 3B). We calculated estimated affinity constants for each scFv variant by applying a saturation binding kinetics model to the ELISA data (GraphPad Prism 9). The peptide modifications did not impact target antigen binding in these constructs, as estimated affinities of the variants were not significantly different from either the unmodified scFv or full-length control (Table 1).

Binding of scFv Variants to FcRn. To evaluate the FcRn-binding properties of our modified scFvs, we constructed a fusion of β2m to the extracellular domain of FcRn. The FcRn–β2m complex binds albumin and IgG Fc in a pH-dependent fashion, with micromolar binding affinity at pH < 6 and minimal binding at pH > 7.[28] FcRnBP–Fc recapitulates this pH-dependent interaction when fused to a fluorescent reporter protein.[19] To generate the FcRn–β2m complex, we fused an *E. coli* codon-optimized human β2m gene to the extracellular domain of human FcRn, connected by a flexible

https://doi.org/10.1021/acschembio.1c00862
ACS Chem. Biol. 2022, 17, 404–413

Table 1. Estimated KD for the Binding of Modified scFvs to HER2

IgG/scFv	calculated K_D (nM)[a]
trastuzumab IgG	1.4 ± 0.3
unmodified scFv	5.6 ± 2.8
V_L-Cyc-V_H	8.5 ± 10
V_L-V_H-Cyc	1.6 ± 0.8
V_L-Lin-V_H	6.1 ± 1.4
V_L-V_H-Lin	2.5 ± 1.9
V_L-Cyc(Y12H)-V_H	2.3 ± 1.5
V_L-Lin(Y12H)-V_H	2.4 ± 1.2
V_L-V_H-Lin(Y12H)	2.9 ± 1.3
V_L-V_H-Cyc(Y12H)	0.7 ± 0.3
V_L-Cyc-V_H-Cyc	2.7 ± 4
V_L-Lin-V_H-CycY12H	6.4 ± 1
V_L-CycY12H-V_H-Lin	9.3 ± 2
V_L-Alb-V_H	0.8 ± 0.2

[a]Binding affinities were calculated using the saturation binding kinetic model in Graphpad Prism. ± denotes the standard error of triplicate samples.

$(Gly_4Ser)_3$ linker and expressed and purified the protein from *E. coli* (Figure 3B). We then evaluated scFv binding to FcRn−β2m by ELISA at both pH values 6 and 7.4. ELISA analysis of scFvs modified with cyclic FcRnBP−Fc, linear FcRnBP−Fc, or FcRnBP−Alb behaved similarly to full-length IgG or albumin (Figure 3C), with estimated K_D values ranging from 0.3 to 1.3 μM at pH 6 (Table 2). Binding affinity at pH 7.4 was too low to be detectable in this assay. The binding of unmodified scFv to FcRn was also undetectable at either pH tested, indicating that the interaction of our scFv variants with FcRn is indeed mediated by their peptide modifications. Neither the acidifying Y12H mutation nor the addition of a second FcRn-binding peptide significantly impacted the binding at pH 6. However, the incorporation of the Y12H mutation did result in a decreased binding at neutral pH. This finding is the expected outcome of replacing tyrosine, which can readily form a hydrogen bond with FcRn, with a pH-titratable histidine that only forms a salt bridge when protonated at low pH (Figure 2D,E).

Table 2. Estimated KD for the Binding of Modified scFv to FcRn at pH 6

IgG/scFv	calculated K_D (μM)[a]
trastuzumab IgG	0.9 ± 0.1
unmodified scFv	ND
V_L-Cyc-V_H	0.2 ± 0.1
V_L-V_H-Cyc	0.3 ± 0.1
V_L-Lin-V_H	0.3 ± 0.1
V_L-V_H-Lin	0.3 ± 0.1
V_L-Cyc(Y12H)-V_H	1.2 ± 0.1
V_L-V_H-Cyc(Y12H)	0.3 ± 0.1
V_L-Lin(Y12H)-V_H	0.05 ± 0.04
V_L-V_H-Lin(Y12H)	0.1 ± 0.1
V_L-Cyc-V_H-Cyc	0.4 ± 0.1
V_L-Lin-V_H-CycY12H	0.4 ± 0.04
V_L-CycY12H-V_H-Lin	0.1 ± 0.03
V_L-Alb-V_H	0.3 ± 0.1
serum albumin	0.3 ± 0.03

[a]Binding affinities were calculated using the saturation binding kinetic model in Graphpad Prism. ± denotes the standard error of triplicate samples.

FcRnBP Modifications Enable FcRn-Mediated Recycling in T84 Cells. Following cellular uptake, albumin and IgG are protected from degradation via pH-dependent binding to FcRn in acidified endosomes and are then trafficked and released either at the surface where they entered (recycling) or at the opposite membrane (transcytosis) (Figure 1A). The recycling pathway is a key driver of the characteristically long serum half-lives of IgG and albumin. Mimicking such interactions should lead to the increased persistence of FcRn-engaging biotherapeutics in the bloodstream via interactions with FcRn-expressing vascular endothelial cells.[29] Additionally, in pharmacodynamically challenging niches such as the gut lumen, where intestinal epithelial cells express FcRn but intravenously administered biotherapeutics do not accumulate to high levels,[30,31] FcRn engagement could support the sustained bioavailability of these drugs following oral dosing or direct gastrointestinal delivery.

To evaluate FcRn-mediated recycling of our scFv variants, we adapted a previously described cell-based assay[32] for use with T84 human colorectal carcinoma cells, which endogenously express FcRn. We incubated T84 monolayers with the following five scFvs, each modified with a single peptide: V_L-Alb-V_H, V_L-Cyc-V_H, V_L-V_H-Cyc, V_L-Lin-V_H, or V_L-V_H-Lin, along with the unmodified scFv and full-length IgG controls. We incubated all samples at pH 5.5 to promote FcRn-mediated retention upon internalization and then washed away non-internalized antibody and incubated overnight at pH 7.4 to allow the internalized antibody (protected from endosomal degradation via binding to FcRn) to be recycled and released into the neutral-pH media, which is nonpermissive for FcRn binding. All scFv variants tested, regardless of peptide position (linker or C-terminal), were recycled at least 2-fold more efficiently than unmodified scFv (Figure 4A), indicating that the enhanced scFv recycling is mediated by the FcRn-binding peptides. Next, to verify that the observed recycling was FcRn-specific, we repeated the recycling assay in the presence of a 30-fold molar excess of competing human IgG or albumin. Recycling of all four FcRnBP−Fc-modified scFvs tested was reduced by 35−60% compared to that of control samples without a competitor added (Figure 4B), supporting the conclusion that recycling of these constructs is FcRn-dependent. Interestingly, similar reductions were not observed for FcRnBP−Alb-modified scFv or full-length IgG, which may be due to differences in FcRn-binding stoichiometry. Because full-length IgG can occupy two FcRn molecules while our peptide-modified scFvs can only occupy one, each molar equivalent of full-length IgG could displace two scFvs but only one IgG, leading to more dramatic reductions in recycling for scFvs compared to IgG. Similarly, both albumin and FcRnBP−Alb-modified scFvs bind FcRn in a 1:1 stoichiometry. Thus, a higher molar excess of competitors may be required to significantly reduce recycling for IgG, albumin, or FcRnBP−Alb−scFv. Competition with the orthogonal full-length protein albumin or IgG did not significantly impact the recycling activity of scFvs modified with FcRnBP−Fc (Figure S1) or FcRnBP−Alb (Figure S2), respectively.

We next investigated the impact of the Y12H-acidifying mutation on the FcRn-mediated recycling of scFvs modified with C-terminal or intralinker FcRnBP−Fc. We observed the significantly increased recycling of cyclic peptide-modified Y12H scFvs at levels 2- to 7-fold higher than full-length IgG

https://doi.org/10.1021/acschembio.1c00862
ACS Chem. Biol. 2022, 17, 404−413

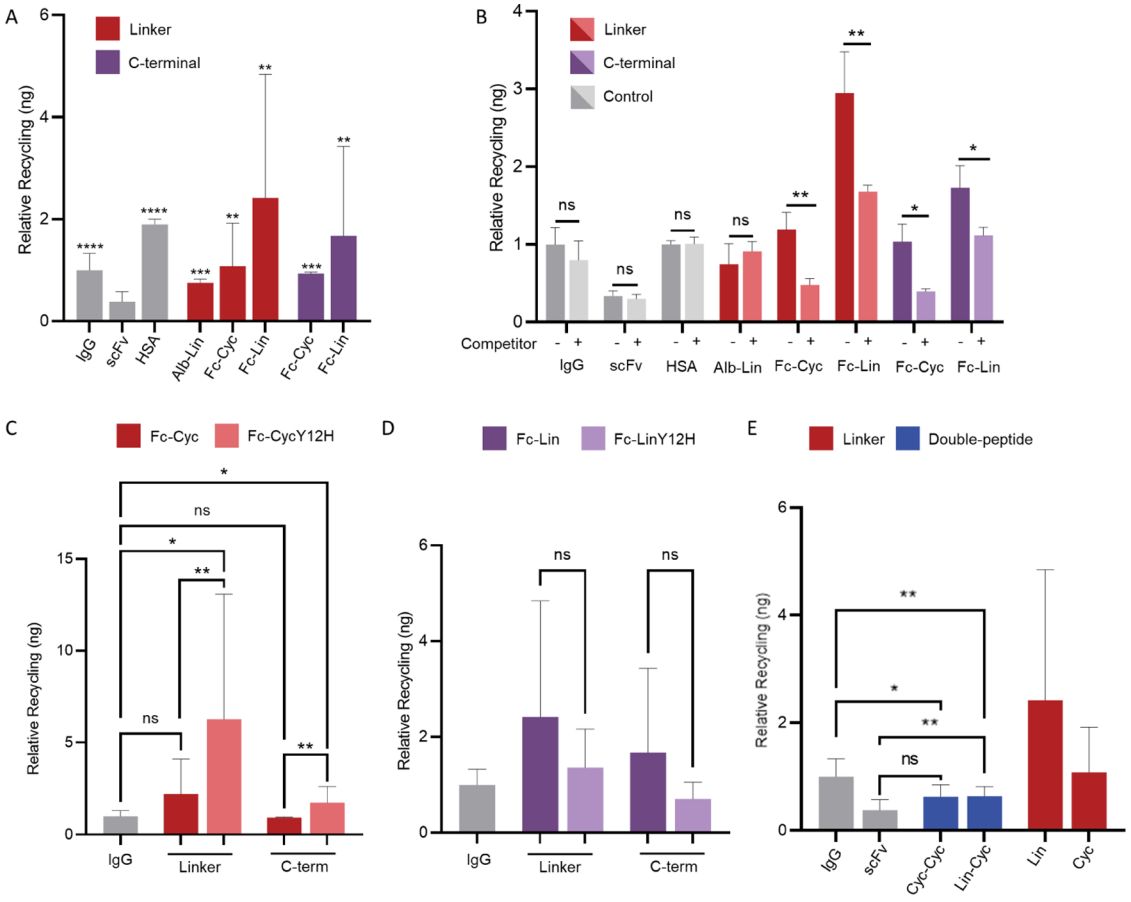

Figure 4. FcRn-mediated recycling of peptide-modified scFvs. (A) Recycling in T84 cell-based assays relative to full-length IgG control. Stars indicate significance over the unmodified scFv negative transport control. (B) Recycling in the presence or absence of 12 μM (30-fold excess) IgG or human serum albumin. Data for scFvs modified with FcRnBP−Fc is presented as ng-recycled, relative to IgG control without the added competitor. Data for scFv modified with FcRnBP−Alb is presented as ng-recycled relative to full-length albumin control without the added competitor. (C−E) Recycling relative to the full-length IgG control of scFvs modified with (C) Cyc or CycY12H FcRnBP−Fc as an intralinker or C-terminal extension, (D) Lin or LinY12H FcRnBP−Fc as an intralinker or C-terminal extension, or (E) two FcRnBP−Fc peptides. All experiments were performed in triplicate. * $0.01 \leq p \leq 0.05$; ** $0.001 \leq p \leq 0.01$; *** $0.0001 \leq p \leq 0.001$; and **** $p < 0.0001$ by two-sided Student's t test in GraphPad Prism 9.

(Figure 4C). The Y12H mutation did not, however, significantly impact the recycling of linear FcRnBP−Fc variants (Figure 4D), which is not surprising considering that computational docking predicted that the distance between peptide histidines and acidic FcRn residues would increase in the Y12H linear FcRnBP−Fc (Figure 2D,E). Finally, we investigated the impact on the recycling activity of incorporating cyclic or linear FcRnBP−Fc peptides at both the linker and C-terminal positions within the same construct and observed moderate increases in activity compared to unmodified scFv but only 60−70% that of the full-length IgG control (Figure 4E).

Notably, structural and functional variations arising from peptide position (C-terminal vs. intralinker), conformation (cyclic vs. linear), or pH sensitivity (parental vs. Y12H mutant) impact the FcRn-mediated activity of the fusion proteins but not equally so. For example, peptide conformation or position alone does not significantly impact recycling activity; whether cyclic or linear, C-terminal or intralinker, all peptides lacking the Y12H mutation failed to increase the recycling efficiency more than ∼1- to 2-fold over unmodified scFvs. However, the acidifying Y12H mutation significantly increased recycling activity over unmodified scFvs by 7- and 4-fold when incorporated at either the intralinker or C-terminal position, respectively, but only with cyclic peptides. In contrast, when incorporated into linear peptides, the Y12H mutation decreased recycling activity, independent of peptide position. Similar results were observed for FcRn-mediated transcytosis of peptide-modified scFvs, with the Y12H mutation leading to a 4-fold increase in activity when added to the VL-Cyc-VH variant and a 5-fold decrease when added to the V_L-V_H-Lin variant.

Our *in silico* structure studies provide insight into the differing effects of the acidifying mutation on the cyclic versus linear FcRnBP−Fc. The histidine residues in question fall at positions 7 and 12 of each peptide, which correspond to positions 121 and 126 for scFvs modified with an intralinker peptide and positions 254 and 259 for scFvs modified with a C-terminal peptide. For both the intralinker and C-terminal cyclic peptides, the histidine residue(s) of the Cyc (His7) and CycY12H (His7/His12) mutants are predicted to be outward-facing and readily available to interact with FcRn residues Asp110 and Glu105 when protonated. It is thus likely that the enhanced recycling and transcytosis activity observed with CycY12H FcRnBP−Fc is due to the additional histidine residue strengthening the interaction with FcRn at pH 6 and

https://doi.org/10.1021/acschembio.1c00862
ACS Chem. Biol. 2022, 17, 404−413

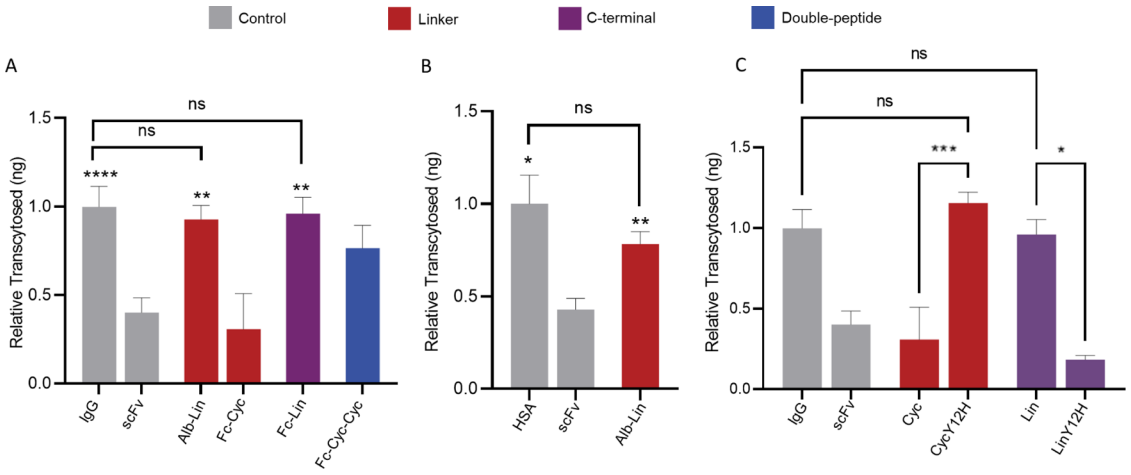

Figure 5. FcRn-mediated transcytosis of peptide-modified scFvs. (A) Transmembrane transcytosis of scFvs modified with FcRnBP−Fc or FcRnBP−Alb, relative to full-length IgG control. Stars indicate significance over the unmodified scFv negative transport control. (B) Transcytosis of scFv modified with FcRnBP−Alb, relative to full-length human serum albumin. Stars indicate significance over the unmodified scFv negative transport control. (C) Transcytosis of scFvs modified with Y12H mutant or nonmutant FcRnBP−Fc, relative to full-length IgG control. All experiments were performed in triplicate. * $0.01 \leq p \leq 0.05$; ** $0.001 \leq p \leq 0.01$; *** $0.0001 \leq p \leq 0.001$; and **** $p < 0.0001$ by two-sided Student's t test in GraphPad Prism 9.

increasing scFv salvage within endocytic vesicles. The inverse is true of the linear FcRnBP−Fc; energy-minimized crystal structures and docking simulations predict an interaction between FcRn Asp110 and His7 of the non-Y12H mutant, whereas the introduction of Y12H leads to a kinked conformation, resulting in both histidines being inaccessible to FcRn (Figure 2B,C).

FcRnBP Modifications Enable FcRn-Mediated Transcytosis in T84 Cells. In addition to FcRn-mediated recycling, IgG and albumin internalized by polarized epithelial and endothelial cells can undergo FcRn-mediated transcytosis, whereby the FcRn-bound proteins are trafficked to the opposite membrane (e.g., apical to basolateral), passing through the cell to cross the otherwise impermeable cell barrier (Figure 1A). Promoting FcRn-mediated transcytosis of biotherapeutics could improve GI bioavailability of systemically administered drugs via blood-to-gut transport[33] or could enable orally delivered drugs to access the systemic circulation and target non-GI conditions. We used an established cell-based assay to quantify the FcRn-mediated transport of peptide-modified scFvs across polarized T84 epithelial cells grown as monolayers on specialized transcytosis inserts.[34] IgG or scFv variants were added to the apical chamber at pH 5.5, and samples were collected from the basolateral chamber 2 h later to quantify transport. For these experiments, we analyzed FcRnBP−Alb as well as the three FcRnBP−Fc variants that performed best in recycling assays, within each of the following categories: single cyclic (V_L-Cyc-V_H), single linear (V_L-V_H-Lin), and dual peptide (V_L-Cyc-V_H-Cyc). Of these, V_L-Alb-V_H and V_L-V_H-Lin were transported at levels equal to full-length IgG and 2- to 3-fold higher than unmodified scFv (Figure 5A). Similarly, FcRnBP−Alb-modified scFvs were transported at ∼80% the level of full-length human serum albumin and 2 times that of the unmodified scFv control (Figure 5B).

Next, we evaluated the impact of the Y12H mutation on FcRn-mediated transcytosis of V_L-V_H-Lin and V_L-Cyc-V_H (Figure 5C). As in the recycling assays, the Y12H mutation enhanced the activity of V_L-Cyc-V_H, resulting in a nearly 4-fold increase in transport with the mutation versus without, and a 20% increase in transport over V_L-V_H-Lin, the best-performing non-Y12H variant (Figure 5A). In contrast, transcytosis decreased by >5-fold for V_L-V_H-Lin upon the addition of the Y12H mutation. As with the recycling assays, the computational docking simulations provide insight into these results. Specifically, CycY12H FcRnBP−Fc likely swaps a hydrogen-bonding tyrosine with a pH-titratable histidine, gaining a pH-dependent salt bridge with FcRn and thus enhanced binding at low pH and decreased binding at neutral pH compared to the non-Y12H variant. Meanwhile, the conformational changes predicted for linear Y12H mutant peptides described in the computational docking studies above likely result in decreased FcRn binding and, subsequently, decreased FcRn-mediated transcytosis activity.

CONCLUSIONS

In this study, we demonstrate that modifying scFvs with small peptide domains mimicking the interaction of IgG or albumin with FcRn enables FcRn engagement and FcRn-mediated recycling and transepithelial transcytosis. Given that IgG Fc and human albumin bind nonoverlapping sites on FcRn, these two classes of peptides could be employed synergistically for multiplexed binding to and increased avidity for FcRn. To the best of our knowledge, this is the first example of modifying antibody fragments with minimal peptide domains to engage FcRn.

Interactions with FcRn help native IgG[13,35] and albumin[20] persist in the circulation. Half-life extension is of particular importance for small antibody fragments, which generally undergo rapid renal excretion, in spite of other advantages including enhanced tissue penetration and superior access to sterically constrained antigens.[36] While a thorough *in vivo* study is required, the cell-based FcRn-mediated transport assays described in this study have previously served as accurate indicators of the *in vivo* performance of antibody fragments.[37] Thus, the observed *in vitro* effects of FcRn-engaging peptides on scFvs may help fully realize the therapeutic potential of antibody fragments. Furthermore, the successful identification and implementation of the albumin-binding domain graft suggests that the structure-guided rational design of small functional peptides for other

https://doi.org/10.1021/acschembio.1c00862
ACS Chem. Biol. 2022, 17, 404−413

protein−protein interactions is readily achievable for incorporation into this platform. While our studies focus on the anti-HER2 scFv, the modularity of the antibody structure should facilitate the portability of peptides between therapeutic scaffolds, and future expansion of the approach could dramatically enhance the therapeutic impact of other small protein therapeutics such as interleukins or enzymes.

Previous work has shown that FcRn engagement enhances gut bioavailability and residence time of IV-dosed antibody fragments via FcRn-mediated blood-to-gut transport.[38] Thus, the modification of antibody fragments with the FcRn-engaging peptides described here could dramatically enhance the impact of these therapeutics against GI targets such as inflammatory bowel disease or recalcitrant *Clostridioides difficile* infection. Further, FcRn engagement has been shown to enable gut-to-blood transport[39] and could facilitate alternative routes of scFv administration including oral dosing, vectored immunoprophylaxis,[40] or *in situ* production by engineered commensal microbes, which have demonstrated promise as delivery vehicles for a host of small protein therapeutics.[41] These delivery methods are attractive alternatives to standard IV or intramuscular administration, which are costly and can lead to serious side effects including infusion site reactions.[42,43] Such advances could also reduce cost and increase access to life-saving antibody-based therapies.[44]

METHODS

Plasmid Construction. All recombinant proteins were expressed using standard methods (see SI). Primers used to construct expression plasmids are listed in Table S1. The gene encoding the extracellular domain (ECD) of HER2 was reverse-transcribed from HEK293T total RNA. The extracellular domain of human FcRn was amplified from a total RNA pool of T84 cells (ATCC CCL-248). All trastuzumab scFv variants, as well as an FcRn−β2m fusion protein, were fused to the signal peptide of *E. coli* outer membrane protein A (OmpA) to promote export to the periplasmic space to facilitate proper disulfide formation.[26]

In Silico Structure Prediction. To generate computational models of scFv antibodies modified with Fc- or albumin-mimetic peptides, the amino acid sequence of each variant was input into the Robetta structure prediction webserver.[45,46] In the case of variants modified with cyclic Fc-mimetic peptides, PDB 3M17[47] was provided as part of the template library for comparative modeling of the peptide domain. Similarly, PDB 1AO6[48] was provided as a potential template for scFvs modified with the albumin-mimetic peptide domain. The models with the lowest estimated angstrom error were selected for further investigation. The Haddock2.2 webserver[24] was then used to simulate the interaction between the FcRn−β2m complex (PDB 4N0U)[22] and the modeled scFv structures. Interacting residues were restricted to the Fc- or albumin-mimetic peptides on the scFvs and the canonical FcRn−IgG and FcRn−albumin-binding interfaces identified in previous crystallography studies.[25] Docking models were selected based on the Haddock best practice guide published at https://www.bonvinlab.org/software/bpg/.

Cellular Recycling and Transcytosis Assays. All cell-based experiments used T84 human colon carcinoma cells (ATCC CCL-248). T84 cultures were maintained in 1:1 DMEM/F12 (Corning) supplemented with 10% (v/v) fetal bovine serum (Thermo Fisher) and 1% (v/v) antibiotic−antimycotic (Gibco) at 37 °C, 5% CO_2. Recycling and transcytosis assays were performed as previously described (Grevys, Foss). Briefly, for recycling experiments, cells were seeded at 2×10^5 cells/well in 48-well cell culture plates (VWR). Once cells reached confluency (~3 days), growth media was aspirated, and cells were starved for 1 h in HBSS at pH 6.0 (Gibco). Antibodies and antibody fragments were diluted to 400 nM in HBSS (pH 6.0) and were incubated with T84 monolayers for 4 h at 37 °C. Antibody solutions were aspirated, and monolayers were washed with cold HBSS at pH 7.4. Cells were then incubated overnight at 37 °C in DMEM/F12 without FBS to facilitate the release of internalized antibodies. Antibody release was detected by ELISA and quantified by comparison to a standard curve of the corresponding purified antibody. For competitive recycling assays, experimental antibodies and antibody fragments were biotinylated with NHS-biotin (ApexBio) according to the manufacturer's instructions and then diluted to 400 nM in HBSS (pH 6.0) containing 12 μM unlabeled human IgG or albumin. Release of biotinylated antibody or antibody fragment was detected by ELISA with streptavidin−HRP (see SI).

For transcytosis assays, cells were seeded at 1.5×10^5 cells/well on 0.4 μm PET transwell inserts (Sterlitech) in 24-well tissue culture plates. Culture media was changed every ~2 days. Transepithelial electrical resistance (TEER) was monitored using a Millicell ERS-2 voltohmmeter (Millipore Sigma). Assays were performed on monolayers exhibiting TEER values of 1000−1500 $\Omega \cdot cm^2$. Once the monolayers polarized, growth media was aspirated and replaced with HBSS at pH 6 (apical chamber) or pH 7.4 (basolateral chamber) for 1 h to starve cells. Full-length antibodies or antibody fragments were labeled with AFDye 488 NHS Ester (Click Chemistry Tools) at 10-fold molar excess as per the manufacturer's instructions. The unreacted dye was removed by desalting on a PD-10 column, and the resulting labeled antibodies were filtered through 0.2 μm PES filters (VWR) before being diluted to 4 μM in HBSS (pH 6) and added to the apical chamber. DMEM/F12 without FBS was added to the basolateral chamber. Fifty microliter samples were collected from the basolateral chamber after 2 h of incubation and loaded into a black 384-well plate (4titude). Transcytosed antibodies or antibody fragments were detected by fluorescence measurement (Ex/Em: 485/528) on a BioTek Synergy HT multimode microplate reader. Sample concentration was estimated using a standard curve of the purified, fluorescently tagged antibody. Wells that had an obvious leak in the monolayer (informed by the abnormally high fluorescence signal in end point assay and subsequent verification via visual inspection of monolayer under 20× magnification) were excluded from analysis.

ASSOCIATED CONTENT

Supporting Information

The Supporting Information is available free of charge at https://pubs.acs.org/doi/10.1021/acschembio.1c00862.

Additional experimental details, primer sequences, and supplemental materials and methods can be found in the Supporting Information (PDF)

AUTHOR INFORMATION

Corresponding Author

Shannon J. Sirk − *Department of Bioengineering, Department of Biomedical and Translational Sciences, Carle Illinois College of Medicine, Carl R. Woese Institute for Genomic Biology, and Cancer Center at Illinois, University of Illinois, Urbana, Illinois 61801, United States*; orcid.org/0000-0001-5424-6813; Phone: 217-300-7413; Email: sirk@illinois.edu

Author

Vince W. Kelly − *Department of Bioengineering, University of Illinois, Urbana, Illinois 61801, United States*

Complete contact information is available at: https://pubs.acs.org/10.1021/acschembio.1c00862

Author Contributions

V.W.K. and S.J.S. designed the research. V.W.K. performed the research and analyzed the data. V.W.K. and S.J.S. wrote the manuscript.

https://doi.org/10.1021/acschembio.1c00862
ACS Chem. Biol. 2022, 17, 404−413

Notes

The authors declare no competing financial interest.

■ ACKNOWLEDGMENTS

This work was supported by institutional startup funding from the University of Illinois Urbana-Champaign and a research grant from the Cancer Center at Illinois. The authors thank the members of the Sirk lab for helpful discussion.

■ REFERENCES

(1) Lu, R.-M.; Hwang, Y.-C.; Liu, I.-J.; Lee, C.-C.; Tsai, H.-Z.; Li, H.-J.; Wu, H.-C. Development of therapeutic antibodies for the treatment of diseases. *J. Biomed. Sci.* **2020**, *27*, No. 1.

(2) Raje, N.; Vallet, S. Sotatercept, a soluble activin receptor type 2A IgG-Fc fusion protein for the treatment of anemia and bone loss. *Curr. Opin. Mol. Ther.* **2010**, 586−597.

(3) Casey, J. L.; Napier, M. P.; King, D. J.; Pedley, R. B.; Chaplin, L. C.; Weir, N.; Skelton, L.; Green, A. J.; Hope-Stone, L. D.; Yarranton, G. T.; et al. Tumour targeting of humanised cross-linked divalent-fab′ antibody fragments: A clinical phase I/II study. *Br. J. Cancer* **2002**, *86*, 1401−1410.

(4) von Minckwitz, G.; Harder, S.; Hövelmann, S.; Jäger, E.; Al-Batran, S. E.; Loibl, S.; Atmaca, A.; Cimpoiasu, C.; Neumann, A.; Abera, A.; et al. Phase I clinical study of the recombinant antibody toxin scFv(FRP5)-ETA specific for the ErbB2/HER2 receptor in patients with advanced solid malignomas. *Breast Cancer Res.* **2005**, *7*, R617−R626.

(5) Sievers, E. L.; Senter, P. D. Antibody-Drug Conjugates in Cancer Therapy. *Annu. Rev. Med.* **2013**, *64*, 15−29.

(6) Huang, C. Receptor-Fc fusion therapeutics, traps, and MIMETIBODY technology. *Curr. Opin. Biotechnol.* **2009**, *20*, 692−699.

(7) Xenaki, K. T.; Oliveira, S.; van Bergen en Henegouwen, P. M. Antibody or antibody fragments: Implications for molecular imaging and targeted therapy of solid tumors. *Front. Immunol.* **2017**, *8*, No. 1287.

(8) Holliger, P.; Hudson, P. J. Engineered antibody fragments and the rise of single domains. *Nat. Biotechnol.* **2005**, *23*, 1126−1136.

(9) Ahmad, Z. A.; Yeap, S. K.; Ali, A. M.; Ho, W. Y.; Alitheen, N. B. M.; Hamid, M. ScFv antibody: Principles and clinical application *Clin. Dev. Immunol.* 2012, *2012*, DOI: 10.1155/2012/980250.

(10) Nelson, A. L.; Reichert, J. M. Development trends for therapeutic antibody fragments. *Nat. Biotechnol.* **2009**, *27*, 331−337.

(11) Yokota, T.; Milenic, D. E.; Whitlow, M.; Schlom, J. Rapid Tumor Penetration of a Single-Chain Fv and Comparison with Other Immunoglobulin Forms. *Cancer Res.* **1992**, *52*, 3402−3408.

(12) Nimmerjahn, F.; Ravetch, J. V. Fcγ receptors as regulators of immune responses. *Nat. Rev. Immunol.* **2008**, *8*, 34−47.

(13) Junghans, R. P.; Anderson, C. L. The protection receptor for IgG catabolism is the β2-microglobulin-containing neonatal intestinal transport receptor. *Proc. Natl. Acad. Sci. U.S.A.* **1996**, *93*, 5512−5516.

(14) Israel, E. J.; Wilsker, D. F.; Hayes, K. C.; Schoenfeld, D.; Simister, N. E. Increased clearance of IgG in mice that lack β2-microglobulin: Possible protective role of FcRn. *Immunology* **1996**, *89*, 573−578.

(15) Möller, R.; Hansen, G. H.; Michael Danielsen, E. IgG trafficking in the adult pig small intestine: One- or bidirectional transfer across the enterocyte brush border? *Histochem. Cell Biol.* **2017**, *147*, 399−411.

(16) Rodewald, R.; Kraehenbuhl, J. P. Receptor-mediated transport of IgG. *J. Cell Biol.* **1984**, *99*, 159s−164s.

(17) Carter, P.; Presta, L.; Gorman, C. M.; Ridgway, J. B.; Henner, D.; Wong, W. L.; Rowland, A. M.; Kotts, C.; Carver, M. E.; Shepard, H. M. Humanization of an anti-p185HER2 antibody for human cancer therapy. *Proc. Natl. Acad. Sci. U.S.A.* **1992**, *89*, 4285−4289.

(18) Mezo, A. R.; McDonnell, K. A.; Hehir, C. A. T.; Low, S. C.; Palombella, V. J.; Stattel, J. M.; Kamphaus, G. D.; Fraley, C.; Zhang, Y.; Dumont, J. A.; et al. Reduction of IgG in nonhuman primates by a peptide antagonist of the neonatal Fc receptor FcRn. *Proc. Natl. Acad. Sci. U.S.A.* **2008**, *105*, 2337−2342.

(19) Sockolosky, J. T.; Tiffany, M. R.; Szoka, F. C. Engineering neonatal Fc receptor-mediated recycling and transcytosis in recombinant proteins by short terminal peptide extensions. *Proc. Natl. Acad. Sci. U.S.A.* **2012**, *109*, 16095−16100.

(20) Chaudhury, C.; Mehnaz, S.; Robinson, J. M.; Hayton, W. L.; Pearl, D. K.; Roopenian, D. C.; Anderson, C. L. The major histocompatibility complex-related Fc receptor for IgG (FcRn) binds albumin and prolongs its lifespan. *J. Exp. Med.* **2003**, *197*, 315−322.

(21) Bern, M.; Nilsen, J.; Ferrarese, M.; Sand, K. M. K.; Gjølberg, T. T.; Lode, H. E.; Davidson, R. J.; Camire, R. M.; Bækkevold, E. S.; Foss, S.; et al. An engineered human albumin enhances half-life and transmucosal delivery when fused to protein-based biologics. *Sci. Transl. Med.* **2020**, *12*, 1−14.

(22) Oganesyan, V.; Damschroder, M. M.; Cook, K. E.; Li, Q.; Gao, C.; Wu, H.; Dall'Acqua, W. F. Structural insights into neonatal Fc receptor-based recycling mechanisms. *J. Biol. Chem.* **2014**, *289*, 7812−7824.

(23) Wang, Z.; Cheng, L.; Guo, G.; Cheng, B.; Hu, S.; Zhang, H.; Zhu, Z.; Niu, L. Structural insight into a matured humanized monoclonal antibody HUA21 against HER2-overexpressing cancer cells. *Acta Crystallogr. Sect. D Struct. Biol.* **2019**, *75*, 554−563.

(24) Van Zundert, G. C. P.; Rodrigues, J. P. G. L. M.; Trellet, M.; Schmitz, C.; Kastritis, P. L.; Karaca, E.; Melquiond, A. S. J.; Van Dijk, M.; De Vries, S. J.; Bonvin, A. M. J. J. The HADDOCK2.2 Web Server: User-Friendly Integrative Modeling of Biomolecular Complexes. *J. Mol. Biol.* **2016**, *428*, 720−725.

(25) Pyzik, M.; Sand, K. M. K.; Hubbard, J. J.; Andersen, J. T.; Sandlie, I.; Blumberg, R. S. The neonatal Fc Receptor (FcRn): A misnomer? *Front. Immunol.* **2019**, *10*, No. 1540.

(26) Baneyx, F.; Mujacic, M. Recombinant protein folding and misfolding in *Escherichia coli*. *Nat. Biotechnol.* **2004**, *22*, 1399−1408.

(27) Sun, Y.; Feng, X.; Qu, J.; Han, W.; Liu, Z.; Li, X.; Zou, M.; Zhen, Y.; Zhu, J. Expression and Characterization of the Extracellular Domain of Human HER2 from Escherichia Coli, and Production of Polyclonal Antibodies Against the Recombinant Proteins. *Appl. Biochem. Biotechnol.* **2015**, *176*, 1029−1043.

(28) Raghavan, M.; Bonagura, V. R.; Morrison, S. L.; Bjorkman, P. J. Analysis of the pH Dependence of the Neonatal Fc Receptor/Immunoglobulin G Interaction Using Antibody and Receptor Variants. *Biochemistry* **1995**, *34*, 14649−14657.

(29) Latvala, S.; Jacobsen, B.; Otteneder, M. B.; Herrmann, A.; Kronenberg, S. Distribution of FcRn Across Species and Tissues. *J. Histochem. Cytochem.* **2017**, *65*, 321−333.

(30) Zhang, Z.; Chen, X.; Hernandez, L. D.; Lipari, P.; Flattery, A.; Chen, S. C.; Kramer, S.; Polishook, J. D.; Racine, F.; Cape, H.; et al. Toxin-mediated paracellular transport of antitoxin antibodies facilitates protection against Clostridium difficile infection. *Infect. Immun.* **2015**, *83*, 405−416.

(31) Dearling, J. L. J.; Park, E. J.; Dunning, P.; Baker, A.; Fahey, F.; Treves, S. T.; Soriano, S. G.; Shimaoka, M.; Packard, A. B.; Peer, D. Detection of intestinal inflammation by MicroPET imaging using a 64Cu-labeled anti-β7 integrin antibody. *Inflamm. Bowel Dis.* **2010**, *16*, 1458−1466.

(32) Grevys, A.; Nilsen, J.; Sand, K. M. K.; Daba, M. B.; Øynebråten, I.; Bern, M.; McAdam, M. B.; Foss, S.; Schlothauer, T.; Michaelsen, T. E.; et al. A human endothelial cell-based recycling assay for screening of FcRn targeted molecules. *Nat. Commun.* **2018**, *9*, No. 621.

(33) Yoshida, M.; Claypool, S. M.; Wagner, J. S.; Mizoguchi, E.; Mizoguchi, A.; Roopenian, D. C.; Lencer, W. I.; Blumberg, R. S. Human neonatal Fc receptor mediates transport of IgG into luminal secretions for delivery of antigens to mucosal dendritic cells. *Immunity* **2004**, *20*, 769−783.

(34) Foss, S.; Grevys, A.; Sand, K. M. K.; Bern, M.; Blundell, P.; Michaelsen, T. E.; Pleass, R. J.; Sandlie, I.; Andersen, J. T. Enhanced FcRn-dependent transepithelial delivery of IgG by Fc-engineering and polymerization. *J. Control. Release* **2016**, *223*, 43−52.

(35) Roopenian, D. C.; Christianson, G. J.; Sproule, T. J.; Brown, A. C.; Akilesh, S.; Jung, N.; Petkova, S.; Avanessian, L.; Choi, E. Y.; Shaffer, D. J.; et al. The MHC Class I-Like IgG Receptor Controls Perinatal IgG Transport, IgG Homeostasis, and Fate of IgG-Fc-Coupled Drugs. *J. Immunol.* **2003**, *170*, 3528−3533.
(36) Labrijn, A. F.; Poignard, P.; Raja, A.; Zwick, M. B.; Delgado, K.; Franti, M.; Binley, J.; Vivona, V.; Grundner, C.; Huang, C.-C.; et al. Access of Antibody Molecules to the Conserved Coreceptor Binding Site on Glycoprotein gp120 Is Sterically Restricted on Primary Human Immunodeficiency Virus Type 1. *J. Virol.* **2003**, *77*, 10557−10565.
(37) Jaramillo, C. A. C.; Belli, S.; Cascais, A. C.; Dudal, S.; Edelmann, M. R.; Haak, M.; Brun, M. E.; Otteneder, M. B.; Ullah, M.; Funk, C.; et al. Toward in vitro-to-in vivo translation of monoclonal antibody pharmacokinetics: Application of a neonatal Fc receptor-mediated transcytosis assay to understand the interplaying clearance mechanisms. *MAbs* **2017**, *9*, 781−791.
(38) Morais, M.; Cantante, C.; Gano, L.; Santos, I.; Lourenço, S.; Santos, C.; Fontes, C.; Aires da Silva, F.; Gonçalves, J.; Correia, J. D. G. Biodistribution of a 67Ga-labeled anti-TNF VHH single-domain antibody containing a bacterial albumin-binding domain (Zag). *Nucl. Med. Biol.* **2014**, *41*, e44−e48.
(39) Stirling, C. M. A.; Charleston, B.; Takamatsu, H.; Claypool, S.; Lencer, W.; Blumberg, R. S.; Wileman, T. E. Characterization of the porcine neonatal Fc receptor - Potential use for trans-epithelial protein delivery. *Immunology* **2005**, *114*, 542−553.
(40) Guilleman, M. M.; Stevens, B. A. Y.; Van Lieshout, L. P.; Rghei, A. D.; Pei, Y.; Santry, L. A.; Thompson, B.; Wootton, S. K. AAV-mediated delivery of actoxumab and bezlotoxumab results in serum and mucosal antibody concentrations that provide protection from C. difficile toxin challenge. *Gene Ther.* **2021**, 1−8.
(41) Kelly, V. W.; Liang, B. K.; Sirk, S. J. Living Therapeutics: The Next Frontier of Precision Medicine. *ACS Synth. Biol.* **2020**, *9*, 3184−3201.
(42) Cheifetz, A.; Mayer, L. Monoclonal antibodies, immunogenicity, and associated infusion reactions. *Mt Sinai J. Med.* **2005**, *72*, 250−256.
(43) Maggi, E.; Vultaggio, A.; Matucci, A. Acute infusion reactions induced by monoclonal antibody therapy. *Expert Rev. Clin. Immunol.* **2011**, *7*, 55−63.
(44) Wellcome, and IAVI. *Expanding Access To Monoclonal Products: A Global Call to Action*, 2020, 1 62.
(45) Raman, S.; Vernon, R.; Thompson, J.; Tyka, M.; Sadreyev, R.; Pei, J.; Kim, D.; Kellogg, E.; Dimaio, F.; Lange, O.; et al. Structure prediction for CASP8 with all-atom refinement using Rosetta. *Proteins: Struct., Funct., Bioinf.* **2009**, *77*, 89−99.
(46) Song, Y.; Dimaio, F.; Wang, R. Y. R.; Kim, D.; Miles, C.; Brunette, T.; Thompson, J.; Baker, D. High-resolution comparative modeling with RosettaCM. *Structure* **2013**, *21*, 1735−1742.
(47) Mezo, A. R.; Sridhar, V.; Badger, J.; Sakorafas, P.; Nienaber, V. X-ray crystal structures of monomeric and dimeric peptide inhibitors in complex with the human neonatal Fc receptor, FcRn. *J. Biol. Chem.* **2010**, *285*, 27694−27701.
(48) Sugio, S.; Kashima, A.; Mochizuki, S.; Noda, M.; Kobayashi, K. Crystal structure of human serum albumin at 2.5 Å resolution. *Protein Eng.* **1999**, *12*, 439−446.

https://doi.org/10.1021/acschembio.1c00862
ACS Chem. Biol. 2022, 17, 404−413